

# Observations of high-frequency internal waves and strong turbulent mixing in a channel flow between two coral atolls

Matthew D. Rayson, Cynthia E. Bluteau, Gregory N. Ivey and Nicole L. Jones

School of Civil, Environmental and Mining Engineering and the Oceans Institute  
University of Western Australia  
35 Stirling Highway, Crawley, Australia, 6009  
\*matt.rayson@uwa.edu.au

## Abstract

Quantifying the physical mechanisms responsible for the vertical fluxes of heat, nutrients, pCO<sub>2</sub> and other tracers is necessary for understanding the vulnerability of coral reef systems to changing ocean conditions and global warming. Preliminary nonhydrostatic numerical modelling around Scott Reef, Australia, an offshore coral atoll system, revealed that a 2 - 3 km wide contraction between the two atolls that comprise Scott Reef leads to barotropic tidal currents in excess of 1 m s<sup>-1</sup> in the 500 m deep channel. Modelling indicates that the associated vertical displacement of isotherms generates internal waves at super-tidal ( $M_4$ ) frequencies and conditions are favourable for an internal hydraulic jump-like feature at the throat of the channel contraction. In April 2015, we deployed two vertical moorings with ADCPs and temperature loggers with resolution  $\Delta z = 20$  m and sampling at  $\Delta t = 0.5$  s and also conducted repeated vertical microstructure profiles near the location of highest internal wave energy. The moorings revealed  $M_4$  tidal frequency isotherm oscillations with peak-to-trough amplitudes of roughly 80 m. Higher frequency oscillations were also prevalent. Following the flood stage of the tide, a high-mode jump-like feature (indicated by rapid isothermal layer separation) occurred around mid-depth. Microstructure measurements revealed typical background turbulent dissipation rates of  $\sim O(10^{-8})$  W kg<sup>-1</sup> that rose to values in excess of  $\sim O(10^{-5})$  W kg<sup>-1</sup> when the jump occurred .

---

## 1 Introduction

Isolated coral atolls and islands are biological hotspots in otherwise oligotrophic ocean environments due to the “Island Mass Effect” (e.g., Gove et al., 2016). Intense vertical mixing associated with tidal friction, island wakes and internal waves is thought to be the dominant driver of enhanced phytoplankton biomass in these island regions. While the connection between increased productivity and island-induced mixing is well established, there are few studies that have actually measured the rates of vertical mixing (although see e.g., Hasegawa et al., 2004; Carter et al., 2006).

Here we present observations from a research cruise to Scott Reef, Australia during April 2015 aboard the R/V Falkor (operated by the Schmidt Ocean Institute). The turbulence observations are put in context with a through water column mooring and results from a 3D nonhydrostatic ocean model, SUNTANS.

## 1.1 Scott Reef Overview

Scott Reef is formed by a pair of coral atolls situated on the edge of the Australian North West Shelf (Figure 1). The two reefs are approximately 40 km in diameter and rise steeply from 500 m depth to the surface. North and South Scott Reef are separated by a 2 - 3 km wide, 500 m deep channel that is the focus of this study. The dominant oceanographic driver is the semi-diurnal barotropic tide with a range of 4 m and barotropic currents up to  $0.2 \text{ m s}^{-1}$  on the shelf waters around Scott Reef (Rayson, 2012; Rayson et al., 2012).

Preliminary nonhydrostatic RANS modelling of Scott Reef produced large amplitude internal waves within this channel that potentially break and drive increased turbulent mixing (Rayson, 2012). The modelling also revealed a bottom-intensified jet with currents in excess of  $1.0 \text{ m s}^{-1}$  between 250 and 400 m below the surface. The strong tidal flow over the steep topography generated transient lee waves characterized by super-tidal frequencies and short horizontal and vertical wave lengths (relative to a linear mode-one internal gravity wave).

## 2 Methods

### 2.1 Numerical Model and Site Selection

A 3D numerical model of the region was used to guide the field site selection and to aid in the interpretation of the observations. We used the SUNTANS ocean model (Fringer et al., 2006), which solves the RANS equations on an unstructured horizontal and fixed z-level vertical grid. A similar model configuration to that described in Rayson (2012) was used with a few key differences, namely, the model was forced with realistic tides (TPXOv7.2), large-scale ocean circulation variables (HYCOM Global 1/12th), and meteorological forcing (ERA-Interim Reanalysis) for the April 2015 period prior to, and during, the cruise (the R/V Falkor has an onboard supercomputer). The grid, with roughly horizontal 79,000 cells and 100 vertical layers, had a resolution  $\Delta x = 250 \text{ m}$  and  $\Delta z = 10 \text{ m}$  near Scott Reef.

Model results were used to target the site of maximum internal wave energy intensity within the channel. We used the method outlined in Rayson et al. (2012) to calculate energy density from the model solution. Figure 1 shows that the semi-diurnal frequency internal wave energy density (sum of kinetic plus potential energy) peaks in magnitude at roughly the throttle point of the contraction in the channel. Consequently, this was where we chose to place the mooring and where the turbulence profiler was deployed.

### 2.2 Description of Observations

Two moorings measuring vertical profiles of temperature, velocity, pressure and salinity were positioned near the 400 m and 200 m isobaths labelled SCR400 and SCR200, respectively in Figure 1. Only data from the SCR400 mooring is presented here. The SCR400 mooring consisted of 19 temperature instruments (SBE56, 39 and 37), six pressure instruments (SBE39P and 37), and two conductivity (SBE37). Velocity in the lower 200 m was measured with a downward looking RDI 75kHz LongRanger, and in the upper 170 m with an upward looking RDI 300 kHz WorkHorse ADCP.

At peak flows, the strong currents led to mooring knockdown in excess of 50 m, which was evaluated via pressure measurements at six locations from 20 m below the surface to 100 m above the seabed. Using six pressure measurements, the temperature observations were then mapped onto a Lagrangian vertical coordinate. ADCP measurements were omitted when the instrument tilt was greater than  $20^\circ$ .

We performed 25 repeated microstructure profiles close to SCR400 to a depth of 200 m over roughly two semi-diurnal tidal cycles using a TurboMAP profiler (Wolk et al., 2002). This instrument measures two components of vertical turbulent shear, fast response temperature and fluorescence at 512 Hz, as well as slow response conductivity, temperature and pressure. Turbulent dissipation rates were computed using the methods outlined in Bluteau et al. (2016). This is the first set of microstructure measurements taken at Scott Reef and one of only a few data sets collected on the entire NWS.

### 3 Results

Temperature oscillations at the SCR400 mooring were characterized by large amplitude displacements (80 m) on the ebb phase of each tidal cycle (negative velocity) and a smaller amplitude upward displacement on the flood phase (Figure 2 a). In addition to a response at the  $M_2$  forcing period, the isotherm displacements had a strong super-tidal ( $M_4$ ) frequency. On several flood cycles, a sharp drop in temperature was observed below 200 m depth. This sharp temperature drop in the lower water column coincided with an asymmetric jet-like current pulse in excess of  $1.5 \text{ m s}^{-1}$  and was followed by high-frequency ( $\omega > N$ ) isotherm oscillations e.g., at  $t = 60$  and  $72$  h in Figure 2 a. These flow attributes are characteristic of transient lee waves that evolve into an internal hydraulic jump on the flood-to-ebb slack phase of the tidal cycle.

The modelled data, shown in Figure 2 b, highlights the shock features and shows the strengthening of the jet-like flow and the associated shocks as the tidal flow increases over the period. Qualitatively, the model captures the key flow features including the bottom-intensified jet,  $M_4$  frequency isotherm oscillations, flood-ebb asymmetry in the current pulse, and the rapid isotherm descent every 12.4 h e.g., at  $t = 35, 47, 60$ , etc. The model does not, however, capture the  $\sim O(N)$  frequency isotherm oscillations after some of the stronger jumps, e.g., at  $t = 60$  h because the length scales of these turbulent processes are smaller than can be resolved by the RANS model ( $\Delta x = 100 \text{ m}$ ,  $\Delta z = 10 \text{ m}$ ).

Displacement spectra for the 12, 15, and 18  $^\circ\text{C}$  isotherms were calculated by linearly interpolating the knockdown-corrected mooring temperature data. These isotherms were located at roughly 250, 200, and 150 m below the surface. As shown in Figure 3, the displacement spectra highlight the significant  $M_4$  ( $2M_2$ ) oscillations. Higher harmonics ( $3M_2$  and  $4M_2$ ) are also present in the 15 and 18  $^\circ\text{C}$  displacement spectra. Such harmonics during internal wave generation are attributable to the nonlinear advection terms, which arise when the internal Froude number and tidal excursion parameter are high, and are also associated with strong turbulent dissipation (e.g., Legg and Huijts, 2006; Musgrave et al., 2016). The spectra observed here show that higher harmonics are being directly and locally generated by the tidal flow through the channel, and suggests an increased likelihood of enhanced small scale mixing.

Turbulent kinetic energy dissipation rate,  $\varepsilon$ , were estimated via repeated microstructure profiles at hourly intervals near the SCR400 mooring (Figure 4). The profiles were

collected over two tidal cycles on April 18 2015 down to a maximum of 200 m below the surface. Background dissipation rates were  $\sim O(10^{-8})$  W kg $^{-1}$ . Several patches of  $\varepsilon > 10^{-6}$  W kg $^{-1}$  appeared around 150 m below the surface at  $t = 1$  and 13 hr in Figure 4 (a). The time-averaged dissipation increases with depth down to roughly 160 m (Figure 4 b). These patches led to peaks in the depth-averaged dissipation of  $1.0-3.0 \times 10^{-6}$  W kg $^{-1}$  during these periods that coincided with the sharp temperature drop and near-bottom jet during flood tide (Figure 4 c).

## 4 Discussion

Through-water column measurements of temperature, velocity, and turbulent dissipation were made in a region of highly nonlinear internal wave generation. Both the topographic slope and the varying width of the channel drive flow divergence and hence isopycnal heaving. This is different from 2D (x-z) flow over a sill where just the topographic slope drives internal wave generation.

Despite the three-dimensional nature of the contraction, the main flow features are consistent with idealized two-dimensional studies of oscillatory flow over a sill (cylinder), namely the near-seabed jet and the generation of internal lee waves (super-tidal frequency internal waves) (e.g., Legg and Huijts, 2006; Winters and Armi, 2013). Winters and Armi (2013) show that these jets form due to a plunging hydraulic layer in the region where the flow transitions from supercritical to subcritical. They also show that these crest-controlled flows are asymmetric, another feature observed in the channel (although this may be a consequence of the asymmetric topography). The important parameter for this class of stratified flow is the layer Froude number,

$$Fr_l = \frac{\bar{U}}{Nh_l},$$

where  $\bar{U}$  is the jet velocity,  $h_l$  is the jet layer thickness, and  $N$  is buoyancy frequency. Based on the SCR400 mooring observations,  $\bar{U} = 1.5$  m s $^{-1}$ ,  $h_l = 150$  m,  $N = 0.01$  s $^{-1}$ ,  $Fr_l = 1$ , meaning the flow is hydraulically-controlled near this point of the contraction during peak flood tide. The  $\sim O(N)$  frequency oscillations in Figure 2 a at  $t = 60$  and 72 h are then likely to be the signature of the type of shear instability predicted by Winters and Armi (2013) in the lee of an object.

The highest TKE dissipation was measured below 150 m at roughly the same time and location as the hydraulic jump events (Figure 4), therefore it is likely we have captured the part of the region of intense mixing with our measurements. In the absence of a strong mean flow, transient lee waves and subsequent jump features due to oscillatory forcing is likely to be the mechanism driving elevated turbulence around isolated island regions like Scott Reef, such as the Northern Great Barrier Reef. Here we have directly observed a hotspot of high turbulent kinetic energy dissipation and probably mixing (if mixing is assumed to be directly correlated with TKE dissipation).

## Acknowledgements

We would like to thank the Schmidt Ocean Institute and the Captain and crew of the R/V Falkor. This data set was collected as part of the Timor Sea Reef Connections Cruise (FK150410). We also thank the Australian Institute of Marine Science, in particular Richard Brinkman and Simon Spagnol for their expertise in the mooring deployment and recovery, Griffith University for the loan of the TurboMap profiler, and David Spencer for guidance with its use. M. Rayson was supported by Stanford University and the Australian Research Council (ARC) Offshore Floating Facilities Research Hub (IH140100012). The field work was funded by the ARC Discovery Project (DP140101322).

## References

- Bluteau, C. E., Jones, N. L., and Ivey, G. N. (2016). Estimating Turbulent Dissipation from Microstructure Shear Measurements Using Maximum Likelihood Spectral Fitting over the Inertial and Viscous Subranges. *Journal of Atmospheric & Oceanic Technology*, 33(1):713–722.
- Carter, G. S., Gregg, M. C., and Merrifield, M. A. (2006). Flow and Mixing around a Small Seamount on Kaena Ridge, Hawaii. *Journal of Physical Oceanography*, 36:1036–1052.
- Fringer, O. B., Gerritsen, M., and Street, R. L. (2006). An unstructured-grid, finite-volume, nonhydrostatic, parallel coastal ocean simulator. *Ocean Modelling*, (October):1–55.
- Gove, J. M., McManus, M. a., Neuheimer, A. B., Polovina, J. J., Drazen, J. C., Smith, C. R., Merrifield, M. a., Friedlander, A. M., Ehses, J. S., Young, C., Dillon, A. K., and Williams, G. J. (2016). Near-island biological hotspots in barren ocean basins. *Nature Communications*, 7:1–34.
- Hasegawa, D., Yamazaki, H., Lueck, R. G., and Seuront, L. (2004). How islands stir and fertilize the upper ocean. *Geophysical Research Letters*, 31(April):2–5.
- Legg, S. and Huijts, K. M. H. (2006). Preliminary simulations of internal waves and mixing generated by finite amplitude tidal flow over isolated topography. *Deep-Sea Research II*, 53:140–156.
- Musgrave, R., Mackinnon, J., Pinkel, R., Waterhouse, A., and Nash J, D. (2016). Tidally Driven Processes Leading to Near-Field Turbulence in a Channel at the Crest of the Mendocino Escarpment. *Journal of Physical Oceanography*, pages 1137–1155.
- Rayson, M. D. (2012). *The Tidally-driven Ocean Dynamics of the Browse Basin and Kimberley Shelf Region, Western Australia*. PhD thesis, University of Western Australia.
- Rayson, M. D., Jones, N. L., and Ivey, G. N. (2012). Temporal variability of the standing internal tide in the Browse Basin, Western Australia. *Journal of Geophysical Research*, 117(C6):C06013.
- Winters, K. B. and Armi, L. (2013). The response of a continuously stratified fluid to an oscillating flow past an obstacle. *Journal of Fluid Mechanics*, 727:83–118.
- Wolk, F., Yamazaki, H., Seuront, L., and Lueck, R. G. (2002). A New Free-Fall Profiler for Measuring Biophysical Microstructure. *Journal of Atmospheric & Oceanic Technology*, 19:780 – 793.

## 5 Figures

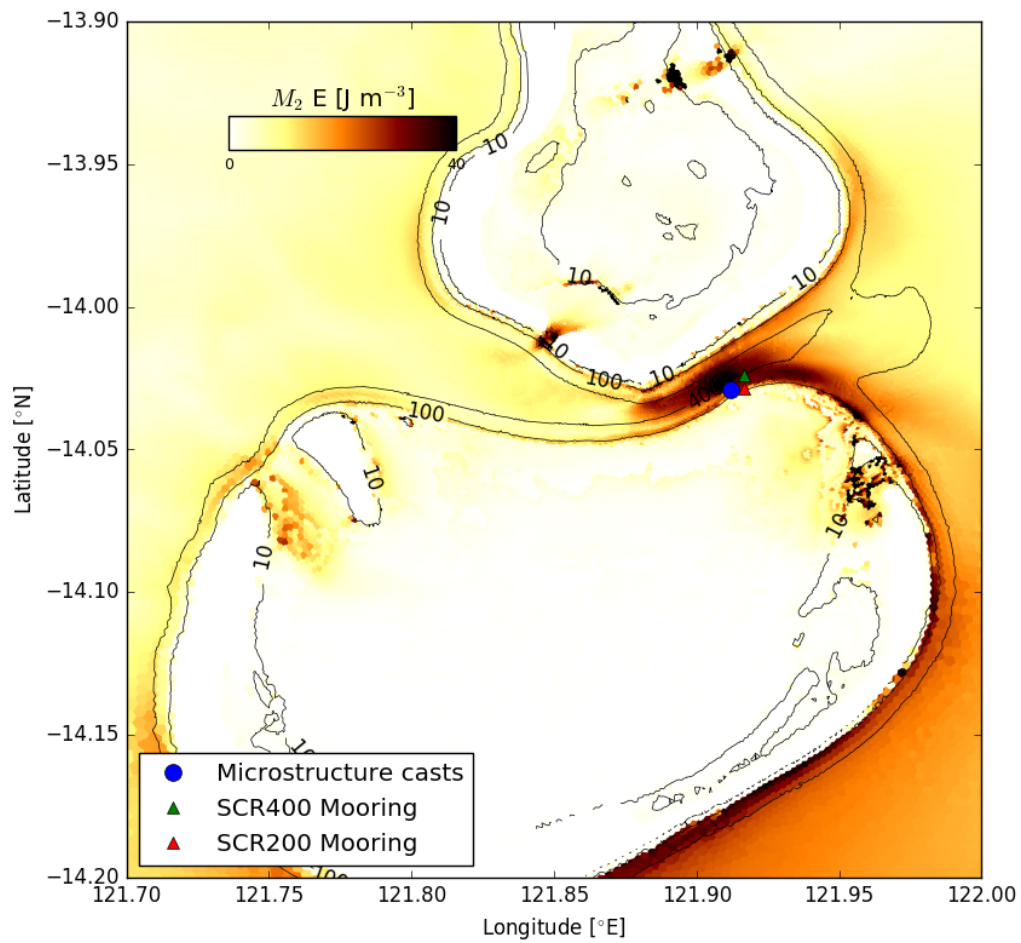


Figure 1: Bathymetric map of Scott Reef with the semi-diurnal frequency internal wave energy density overlaid. Mooring and microstructure locations used in this paper are also indicated.

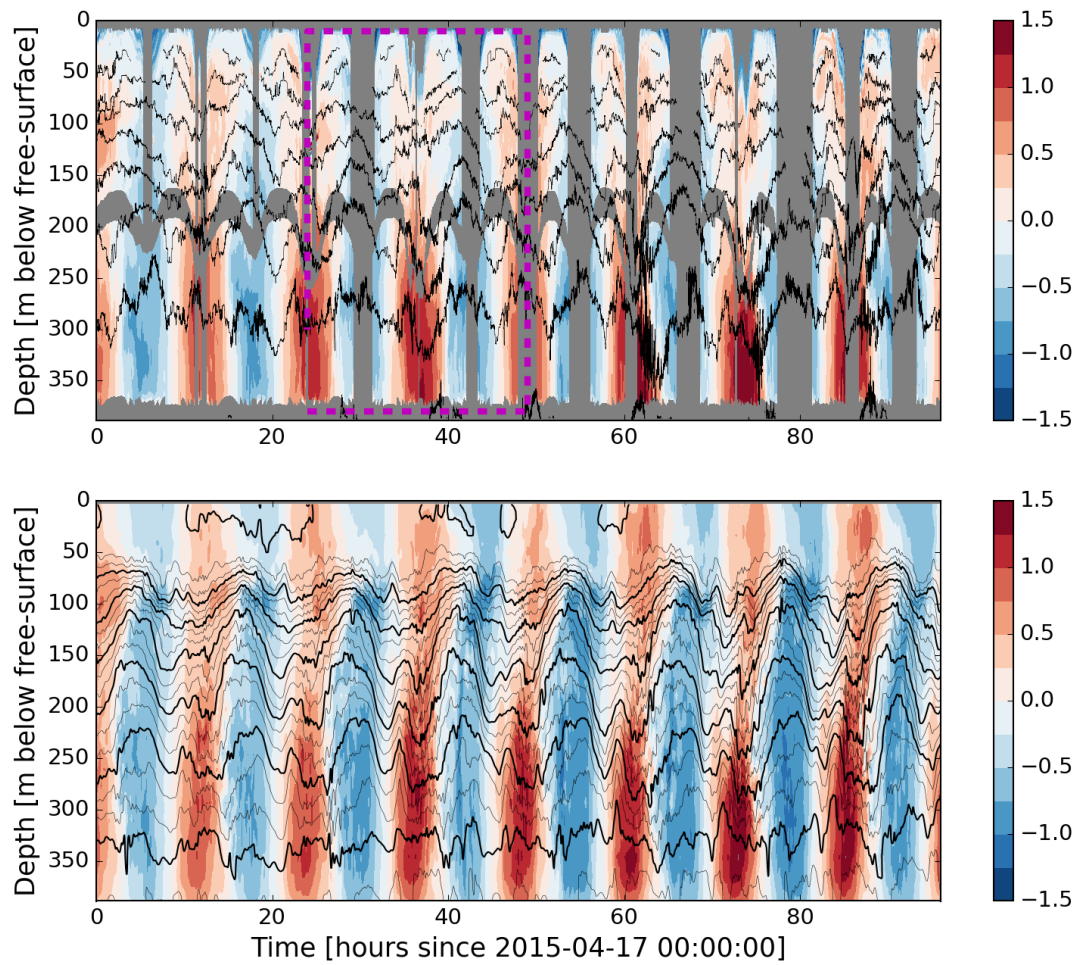


Figure 2: (top) Measured eastward velocity ( $\text{m s}^{-1}$ ) with water temperature contours overlaid at the 400 m mooring, and (bottom) the  $\Delta x = 100$  m nonhydrostatic SUNTANS prediction at the same site. Isotherm intervals are  $3\text{ }^{\circ}\text{C}$  and  $1\text{ }^{\circ}\text{C}$  for the thick and thin lines, respectively. The pink dashed box indicates the time period when microstructure profiles were taken.

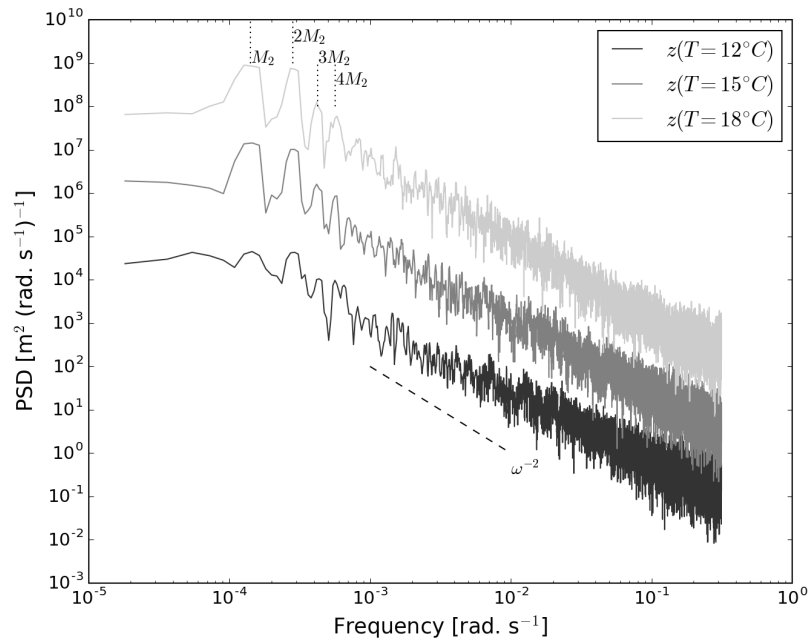


Figure 3: Displacement spectra of the 12, 15 and 18 °C isotherms at the 400 m mooring. The 12 and 18 °C spectra are offset by plus and minus two decades, respectively.

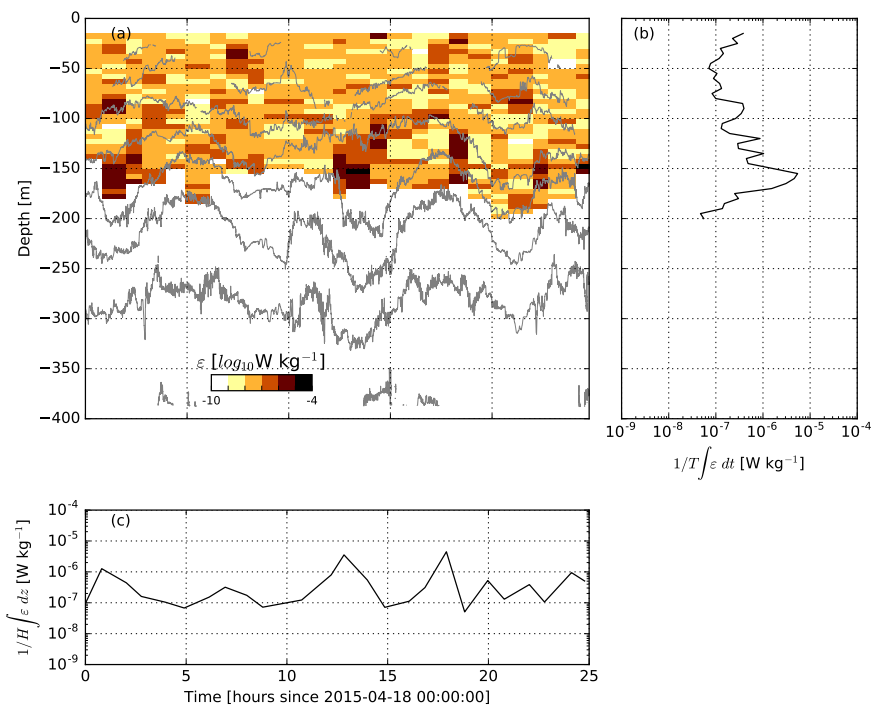


Figure 4: (a) 5 m bin-averaged, (b) time-averaged, and (c) depth-averaged turbulent dissipation rate,  $\varepsilon$ , at the 24 hour microstructure station. Isotherms at 3 °C intervals from SCR400 are overlaid for context.